Infinite Science | Publishing

Laser weldability of laser powder bed fused AlSi7Mg0.6

K. K. Yetil[1*], S. D'Arcangelo[1], B. Previtali[1], and A. G. Demir[1]

[1] Department of Mechanical Engineering, Politecnico di Milano, Milan, Italy
[*] Corresponding author, email: kenankaan.yetil@polimi.it

Abstract

Laser Powder Bed Fusion (LPBF) allows to manufacture components with lightweight and near net shape suited to aerospace and aviation applications employing Al-alloys. The process is highly suited to one-of-a-kind or small batch production of small to medium sized parts. As the maturity of the process and its end-users increase, the demand for larger components becomes more relevant. The increase of part size by increasing the size of the LPBF machine inevitably increases the cost and the complexity of the employed system. Moreover, using multiple lasers in a large powder bed to produce larger parts may bring residual stresses, part deformation and a higher chance of process failure. In the light of these, the use of joining operations, in particular welding, appears as a suitable option for the production of large components via LPBF. Indeed, the process lends itself well to also producing dedicated joint edge preparations, thickness and section variation within the location of the welded joint. Amongst different processes, laser welding stands out as a viable option as it can provide narrower weld seam and heat affected zone, produce less deformation on the parts and be automated with cartesian or robotic manipulators. This work discusses the influence of different laser welding strategies on the LPBF produced AlSi7Mg0.6.

Keywords: Laser Welding, LPBF, AlSi7Mg0.6, Pore Formation, Beam Oscillation

1. Introduction

Laser Powder Bed Fusion (LPBF) technology enables the construction of highly complex 3D parts through the use of laser beam to process metallic powders in a layer-by-layer fashion. With its capability to produce highly customized parts with detailed features and good mechanical properties, LPBF technology has been playing a significant role in industries like aerospace, biomedical and mold and die [1, 2]. Several aspects of LPBF technology were studied and contributions made in process powders, multi-material processing, melt pool sensing, overhang and support structures, baseplate preheating, novel laser beam shaping and remelting strategies [3–7]. In light of all these contributions, LPBF technology has been maturing rapidly, however, one technology limitation is yet to be overcome; built size.

With the commercialization of larger LPBF machines with multiple lasers, this technological limitation has been partially addressed. Nevertheless, utilizing larger machines has its economic and technical drawbacks. In addition to the increased capital expenditure, powder handling, maintaining an inert process chamber, process times, scan head calibrations, and thermal distortions are some of the challenges.

Another approach to overcoming size limitation can be through the assembly and joining of LPBF parts. Consequently, this approach allows for the parallel production of sub-parts using relatively smaller and easy-to-handle LPBF machines, which can then be joined together to form larger parts. Among the various assembly and joining techniques, laser welding is particularly significant owing to its similarity to LPBF in terms of know-how, as well as its robustness, speed, and adaptability to automation.

In the literature, laser weldability of some LPBF produced alloys such as stainless steel, titanium and Inconel have been studied, and relatively successful welds with low relative densities were obtained [8–10]. However, as being one of the most commonly used materials in aerospace, automotive and aviation industries, laser welding of LPBF produced aluminium alloys still requires a greater understanding. Various researchers made efforts on the laser weldability of the LPBF produced aluminium alloys, and the biggest challenge emerged as significantly high percentage of porosity, hence poor mechanical properties [11–16].

While the previous results provide an overview of the problem, a deeper understanding of the causes of pore formation is necessary. From this perspective, the use of more recent solutions, such as beam oscillation and wire feeding, also seems to have been neglected. In fact, beam oscillation (wobbling) has been demonstrated to effectively reduce porosity in laser-welded conventional aluminium alloys by inducing a degassing action [17]. Moreover, the use of a filler wire can help compensating such issue by regulating the chemical composition in the weld pool.

2. Material and methods

In this work, laser weldability of LPBF produced AlSi7Mg0.6 is assessed with novel beam oscillation and wire feeding solutions. Flat plate specimens with 50 mm x 75 mm x 3 mm dimensions were produced using

gas atomized AlSi7Mg0.6 powder with particle size ranging between 20-60 μm. LPBF system used in the present work was Renishaw AM250. Using already optimized parameters, as seen Table 1, plates with relative densities over 99% were produced.

Table 1. Process parameters used for LPBF of AlSi7Mg0.6.

LPBF Process Parameters	Value
Power, W	200
Beam diameter, μm	70
Hatch distance, μm	139
Layer thickness, μm	25
Point distance, μm	88
Exposure time, μs	131
Pre-heating	None

Produced specimens were welded using a robotized laser welding system (BLM Group Adige Alfetta). The processing beam was a continuous wave infrared laser with a maximum power output of 6000 W with a 100 μm processing fiber (IPG Photonics YLS-6000). As seen in Fig. 1(a), the laser system was equipped with a 6 degree of freedom ABB IRB 4600 robotic arm with ABB IRPB A-250 rotary-tilting table. The welding head encased two galvanometric scanners that are able to oscillate the beam in various shapes, while the beam was collimated with a 100 mm and focused with a 150 mm lens (IPG Photonics D50 Wobbling Head). The wobbling head allowed to increase the weld pool by oscillating the beam in a circular pattern with certain frequency and amplitude values. On the other hand, as seen in Fig. 1(b), the effect of the filler wire was investigated using an Al 5356 filler wire, which is commonly used for welding of AlSiMg alloy compositions, with a diameter of 1.2 mm. The filler wire was fed using a wire feeder (Abicor Binzel MFS-V3) and all welds were shielded using an Argon flow.

Initially, full pass weld conditions were sought in a bead on plate configuration comparing beam oscillation and wire feeding solutions opposed to autogenous laser beam welding without oscillation. Fig. 2 shows representative welds obtained using oscillating and stationary beams with and without the filler wire. The welding conditions were analysed measuring the optical densities and further analysed via EDX to understand the cause of the excessive porosity.

Table 2. Experimental campaign carried along with fixed and varied parameters during the bead on plate laser welding of LPBF produced AlSi7Mg0.6.

Fixed Parameters	Value
Beam spot diameter, ds, μm	432
Inert gas & flow rate, l/min	Argon, 20
Head inclination	5°
Varied Parameters	
Beam oscillation	None; Circular with f=40 Hz, A=2 mm
Laser power, P (kW)	3; 3.5
Weld speed, V (m/min)	1.5; 2
Wire speed, WFR (m/min)	0; 1

As it can be seen in Table 2, in order to elaborate on the efforts on the laser weldability of LPBF produced AlSi7Mg0.6, stationary and oscillating beams were compared varying laser power, weld speed and wire speed. Essentially, a 2^k factorial design with a central point was created and executed for each beam condition.

Next, the possible improvement effect of gap in the butt-joint configuration was investigated. The motive of the gap was to decrease the melt fraction of the LPBF produced material in the weld by the use of wire. In this way, most of the laser energy could be absorbed by the wire and a gap could make sure a lesser direct interaction between laser and the base material. Table 3 reports the employed parameter combinations to 6.6 m/min to bridge the considerably large gap in this exploratory phase.
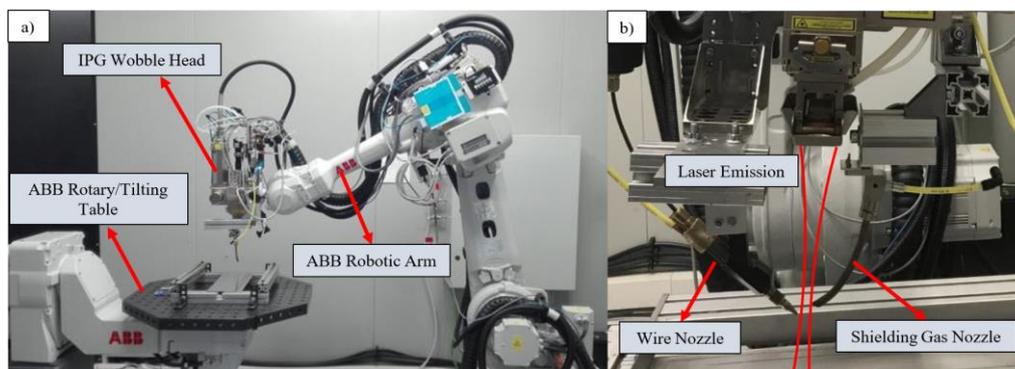

Fig 1. Welding system consists of a) robotic and beam oscillation units, and b) wire feeding and shielding.
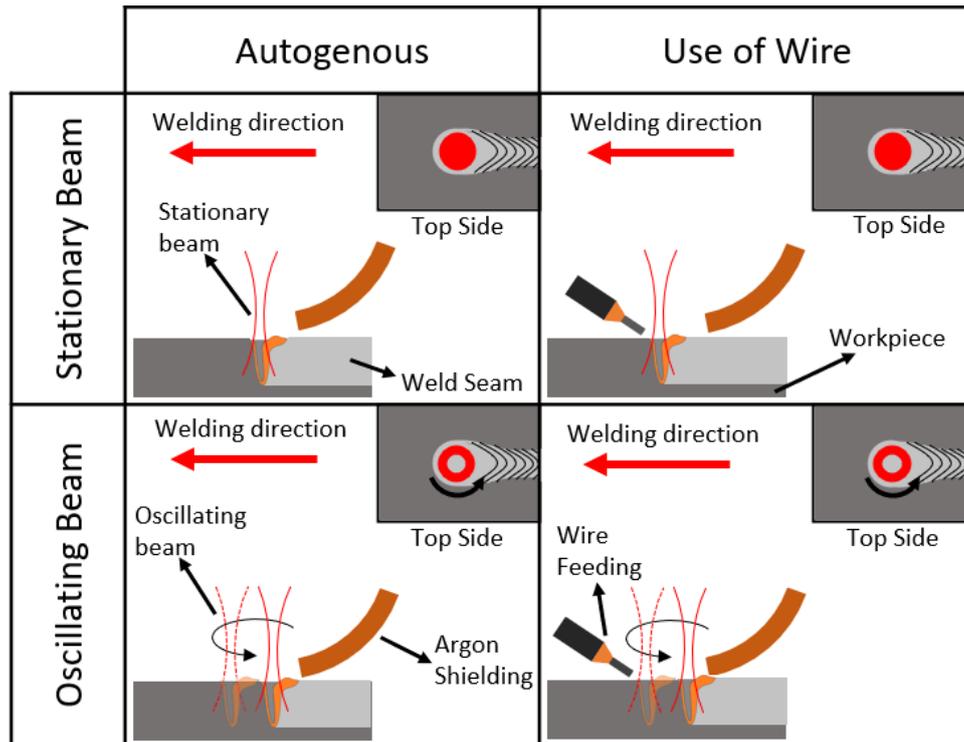
Fig 2. Representative bead on plate weld conditions.

The laser spot size was decreased to 385µm, while increasing the wire speed between the plates. The beam oscillation was circular with 70 Hz frequency and a varying amplitude between 1 and 2 mm. The laser power was adjusted between 1.50 and 2.25 kW.

Table 3. Process parameters used during the butt-welding experiments of LPBF produced AlSi7Mg0.6.

Fixed Parameters	Value
Beam spot diameter, ds, µm	385
Inert gas & flow rate, l/min	Argon, 20
Head inclination	5°
Wire speed, WFR (m/min)	6.6
Weld speed, V (m/min)	1.5
Varied Parameters	
Beam oscillation	Circular with f=70 Hz, A=1-2 mm
Laser power, P (kW)	1.50-2.25

3. Results and discussion

3.1. Bead on plate welds

Fig. 3 shows the cross-section images of the obtained welds. Welds with porous cross sections were obtained under both beam conditions. At first glance, it is apparent that all the pores are spherical in shape indicating gas inducement. In addition, oscillating beam, i.e., oscillation amplitude, brought wider top and root widths. On the other hand, due to the nature of the circular oscillation, the pores seem to be pushed to the sides of the welds. The porosity levels did not change significantly as a function of the process parameters. The maximum optical relative densities obtained after binarizing the images were reported as 66.2% for the stationary beam and 65.8% for the oscillating beam.

SEM/EDX analyses were conducted to further the understanding of pore formation. A line analysis was carried out in two directions, as shown in Fig. 4(a), to identify the alloying and contaminating elements in the base material. In order to have an idea on the elemental content in a weld, 10 different point analyses were performed along the circumference of a pore. As indicated with red crosses in Fig. 4(b), 5 of 10 measurements were done just outside and the remaining 5 were done just inside the pore.

The results of SEM/EDX analysis are reported in Fig. 5, which was constructed based on the mean weight percent of the most prominent elements and their standard deviations. For a better demonstration of all the elements, the left vertical axis of the graph is attributed to the mean weight percent for aluminium content while the right vertical axis of the graph is attributed to the mean weight percent for silicon, magnesium and oxygen contents. It can be observed that the oxygen content inside the pore (11.7%) is significantly higher than the content of the base material and the outside the pore. Additionally, the standard deviations for the elements are larger for the weld compared to the base material. Finally, significant oxygen content can be noticed in the base material, despite of its relatively large standard deviation, which

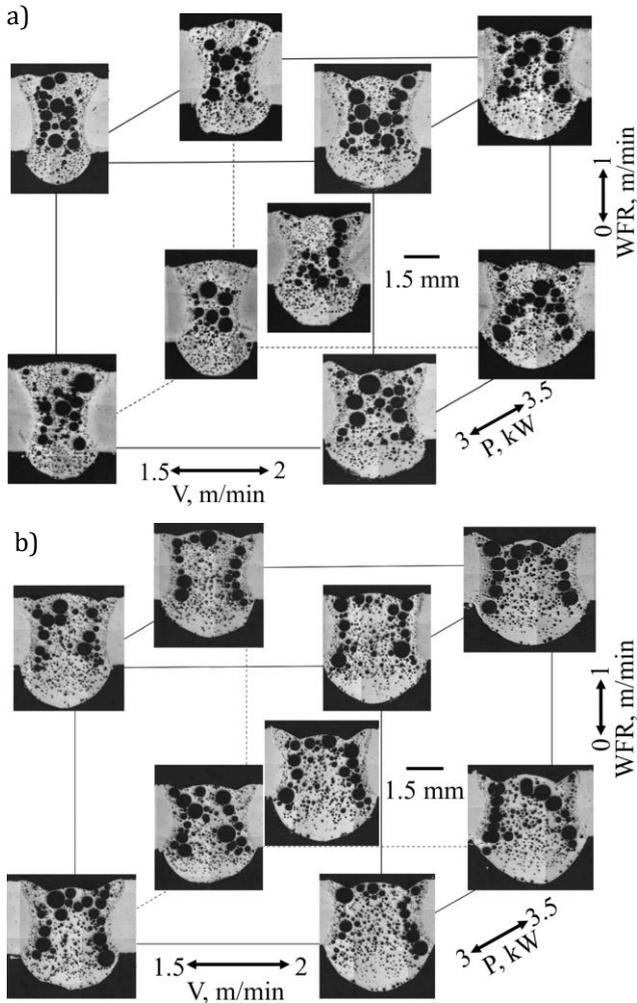may be an indication of the oxidation of the powder feedstock.

a)

b)

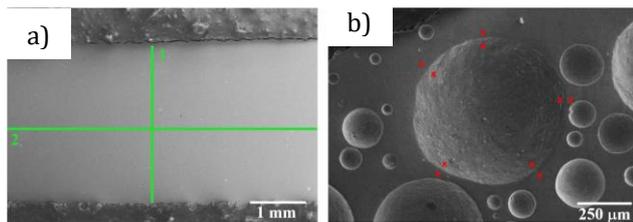**Fig 3.** Weld cross sections achieved with a) stationary beam and b) oscillating beam.

Fig 4. a) Scanning electron microscopy (SEM) image of the base material, b) SEM image of one of the pores in a weld (Oscillating beam; P = 3.5 kW; WFR = 1 m/min; V = 2 m/min).

SEM/EDX results suggest oxygen accumulation around the pore regions indicating a strong chemical composition variation. The oxygen or hydrogen intake can occur during the laser welding, while in conventionally produced Al-alloys such high porosity levels do not commonly appear. Hence, the observed spherical and large pores may have formed due to coalescence of the oxygen intake that may have occurred during the LPBF as also suggested by the following researchers [11]. In the light of these, to decrease the rate of the chemical reaction, a preliminary

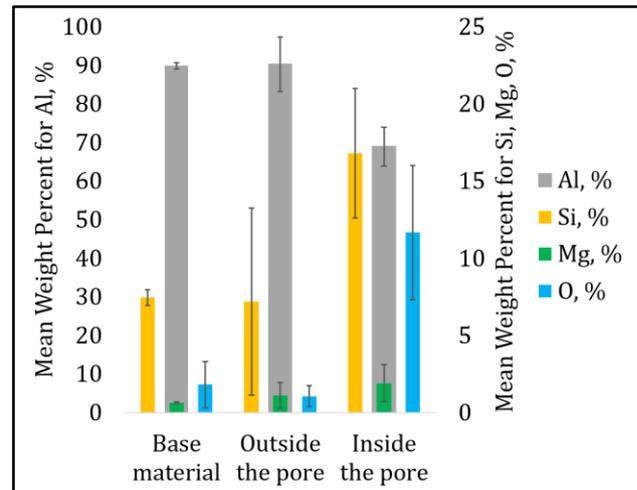experiment was made by decreasing the direct heat input coming from the laser onto the base material.

Fig 5. Energy-dispersive x-ray spectroscopy (EDX) results of the base material and the welds.

3.2. Butt-joint welds with 1 mm gap

Fig. 6 demonstrates the produced welds with 1 mm gap. Noticeably, as the power and the amplitude decreased, the number of pores decreased significantly. Relative densities of 98.3% (Figure 6(b) and 91.4% (Figure 6(c)) were achieved for partial and full penetration butt welds, respectively. While a relative density of 97.4% was achieved for weld e) in Figure 6, it should be noted that the correct joining action was not fulfilled due to low power and small amplitude. The results indicate that further adjustments to the gap and wobbling parameters could lead to a reduction in porosity while maintaining an adequate melting condition.
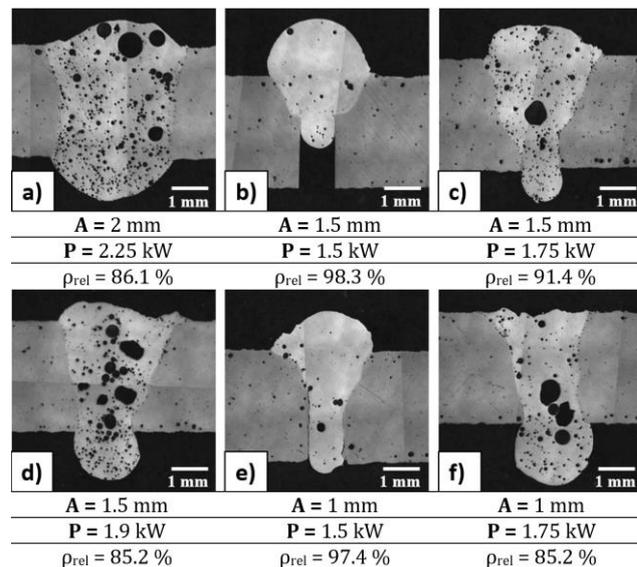

A = 2 mm	A = 1.5 mm	A = 1.5 mm
P = 2.25 kW	P = 1.5 kW	P = 1.75 kW
ρ_{rel} = 86.1 %	ρ_{rel} = 98.3 %	ρ_{rel} = 91.4 %
A = 1.5 mm	A = 1 mm	A = 1 mm
P = 1.9 kW	P = 1.5 kW	P = 1.75 kW
ρ_{rel} = 85.2 %	ρ_{rel} = 97.4 %	ρ_{rel} = 85.2 %

Fig 6. Cross sections of the butt welds with 1 mm gap performed, their relative process parameters and relative density values (ρrel).

Infinite Science | Publishing

Table 4. Some laser welding results of LPBF produced AlSi alloys in the literature compared to the present work.

Material	Thickness, mm	Beam oscillation	Use of wire	Joint type	Gap	Weld atmosphere	Relative density, %	References
AlSi7Mg0.6	3	Present	Present	Butt	1 mm	Atm.	91.4	Present work
AlSi7Mg0.6	2	None	None	Butt	None	Atm.	76	[14]
AlSi10Mg0.6	2	Present	None	Butt	None	Atm.	93.5	[15]
AlSi10Mg	3	None	None	Butt	None	Atm.	93	[16]

As seen in Table 4, in the literature, the amount of works concerning the laser welding of LPBF produced AlSi alloys are very limited. In terms of the relative densities, the present work offers comparable results while being the sole work investigating the effect of the gap.

4. Conclusions

In this work, the efforts were made in order to deepen our grasp on the laser welding of LPBF manufactured AlSi7Mg0.6 using novel beam oscillation and wire feeding. By making a series of welds, cross section and semi-quantitative analyses, the following points can be inferred:

- For bead on plate welds of LPBF produced AlSi7Mg0.6, the use of wire and oscillation appears to be redundant.
- The oxygen content inside the pore is significantly high. Such high oxygen content is attributed to the oxidation in LPBF produced material and inherently from the powder feedstock due to high specific area of the powder grains.
- The novel beam oscillation technique and wire feeding solution may be a remedy for the excessive pore formation for butt joints with a gap. As seen in Figure 6(b) and (c), in the case of double sided or partial penetration welds, the present technique can offer relative densities up to 98.3%.
- Considering the nature of any welding process of complex parts, gaps are almost always present due to differences in the tolerances of the parts to be welded. From this perspective, the current work proposes a robust solution for avoiding quality deviations along the weld seam by considering the effect of a gap.

Overall, with the current laser welding solutions, pore formation seems to be inevitable for LPBF produced AlSi alloys. From this point on, the future efforts will concentrate on different oscillation techniques and joint types to improve the relative density of the welds as well as studies on mechanical properties.

Author's statement
Conflict of interest: Authors state no conflict of interest. Informed consent: Informed consent has been obtained from all individuals included in this study. Ethical approval: N/A.

References
1. B. Ergene, Simulation of the production of Inconel 718 and Ti6Al4V biomedical parts with different relative densities by selective laser melting (SLM) method. Journal of the Faculty of Engineering and Architecture of Gazi University, 2022, 37(1): p. 469–484.
2. C. Tan et al., Design and additive manufacturing of novel conformal cooling molds. Materials and Designs, 2020, 196.
3. E. Vasileska, A. G. Demir, B. M. Colosimo, and B. Previtali, A novel paradigm for feedback control in LPBF: layer-wise correction for overhang structures. Advances in Manufacturing, 2022, 10(2), p. 326–344.
4. L. Caprio, A. G. Demir, G. Chiari, and B. Previtali, Defect-free laser powder bed fusion of Ti–48Al–2Cr–2Nb with a high temperature inductive preheating system. Journal of Physics: Photonics, 2020, 2(2).
5. F. Galbusera, L. Caprio, B. Previtali, and A. G. Demir, The influence of novel beam shapes on melt pool shape and mechanical properties of LPBF produced Al-alloy. Journal of Manufacturing Processes, 2023, 85, p. 1024–1036.
6. M. Colopi, A. G. Demir, L. Caprio, and B. Previtali, Limits and solutions in processing pure Cu via selective laser melting using a high-power single-mode fiber laser. International Journal of Advanced Manufacturing Technology, 2019, 104(5–8), p. 2473–2486.
7. B. Yalçın, U. Karakılınç, and B. Ergene, Investigation on the suitability of powder particulars used in powder bed/feed additive manufacturing and powder manufacturing methods. Journal of Polytechnic, 2018.
8. T. Jokisch, A. Marko, S. Gook, Ö. Üstündag, A. Gumenyuk, and M. Rethmeier, Laser welding of SLM-manufactured tubes made of IN625 and IN718, Materials, 2019, 12(18).
9. W. W. Wits and J. M. Jauregui Becker, Laser beam welding of titanium additive manufactured parts, In Procedia CIRP, 2015, 28, p. 70–75.

10. V. P. Matilainen, J. Pekkarinen, and A. Salminen, Weldability of additive manufactured stainless steel. In Physics Procedia, 2016, 83, p. 808–817.
11. C. Zhang et al., A comparison between laser and TIG welding of selective laser melted AlSi10Mg. Optics and Lasers Technology, 2019, 120.
12. B. Möller, K. Schnabel, M. Scurria, A. Jöckel, and J. Baumgartner, Fatigue assessment of laser beam welds between AlSi10Mg AM-structures and conventionally manufactured aluminum by local approaches. Procedia Structural Integrity, 2021, 34, p. 160–165.
13. J. Mäkikangas, T. Rautio, A. Mustakangas, and K. Mäntyjärvi, Laser welding of AlSi10Mg aluminium-based alloy produced by Selective Laser Melting (SLM). In Procedia Manufacturing, 2019, 36, p. 88–94.
14. V. Dimatteo, E. Liverani, A. Ascari, and A. Fortunato, Weldability and mechanical properties of dissimilar laser welded aluminum alloys thin sheets produced by conventional rolling and Additive Manufacturing. Journal of Materials Processing Technology, 2022, 302.
15. C. Zhang et al., A comparison between laser and TIG welding of selective laser melted AlSi10Mg. Optics and Lasers Technology, 2019, 120.
16. L. Cui et al., Porosity, microstructure and mechanical property of welded joints produced by different laser welding processes in selective laser melting AlSi10Mg alloys. Optics and Lasers Technology, 2022, 150.
17. D. M. Boldrin, M. Colopi, S. D'arcangelo, L. Caprio, A. Gökhan Demir, and B. Previtali, High speed videography of gap bridging with beam oscillation and wire feeding during the laser welding of stainless steel and aluminum alloys. In Lasers in Manufacturing Conference, 2021.